ICF100749OR

FIRST-PRINCIPLES CALCULATIONS OF THE TENSILE STRENGTH AND FRACTURE OF COINCIDENCE TILT BOUNDARIES IN SiC

M. Kohyama

Interface Science Research Group, Special Division of Green Life Technology,
National Institute of Advanced Industrial Science and Technology,
Ikeda, Osaka 563-8577, Japan

ABSTRACT

Ab initio tensile tests have been applied to the polar and non-polar interfaces of the {122}Σ=9 coincidence tilt boundary in cubic SiC, where the tensile strength and fracture have been examined through the behavior of electrons and atoms based on the density-functional theory. The tensile strength of these interfaces is very large and over 80% of that of bulk crystal, because of the reconstruction of interfacial bonds. However, the presence of the interfacial C–C and Si–Si wrong bonds seriously affect the strength and fracture. The N-type polar interface with C–C bonds is the strongest. For the non-polar interface with both C–C and Si–Si bonds, the fracture starts from the back Si–C bond of the C–C bond because of local stress concentration at the atomic scale, and the fracture proceeds from bond to bond rather continuously. The P-type polar interface with Si–Si bonds does not reveal remarkable local stress concentration, because of the highly symmetric configuration. Thus this interface is stronger than the non-polar one, and the fracture occurs rather catastrophically. For the Si–C bond breaking, we have found the general critical bond stretching dominating the criterion of the fracture.

KEYWORDS

SiC, grain boundary, coincidence boundary, first-principles calculation, tensile strength, fracture, electronic structure

INTRODUCTION

SiC is a very important material as a high-performance ceramic. Grain boundaries dominate various properties of SiC ceramics. The understanding of mechanical properties of SiC grain boundaries is of great importance. For this purpose, it is essential to examine the behavior of grain boundaries under various tensile or shear stresses. In covalent materials like SiC, such mechanical behavior should be seriously dominated by the behavior of both electrons and atoms. Currently, by virtue of the development of the first-principles molecular-dynamics method [1] based on the density-functional theory [2], such complicated problems can be dealt with theoretically [3] in a similar way to recent theoretical studies of the mechanical behavior of bulk crystals [4,5] and defects [6]. In this paper, we investigate the tensile

strength and fracture of a coincidence tilt boundary in cubic SiC theoretically through the behavior of electrons and atoms [7].

THEORETICAL METHOD

We deal with the {122}Σ=9 boundary in cubic SiC. This is a typical coincidence tilt boundary frequently observed in chemical vapour-deposited SiC [8]. Two polar and one non-polar interfaces can be constructed by inverting the polarity of each grain as shown in Fig. 1 [9]. In each model, all the interfacial atoms are four-fold coordinated similarly to the same boundary in Si, and two sets of five-membered and seven-membered rings constitute one period along the ⟨411⟩ direction. However, the polar interfaces are non-stoichiometric and the non-polar interface is stoichiometric. The N-type polar interface contains two C–C wrong bonds and two interfacial Si–C bonds per period, although the P-type polar interface contains two Si–Si wrong bonds and two interfacial Si–C bonds per period. The non-polar interface contains both C–C and Si–Si wrong bonds and two interfacial Si–C bonds.

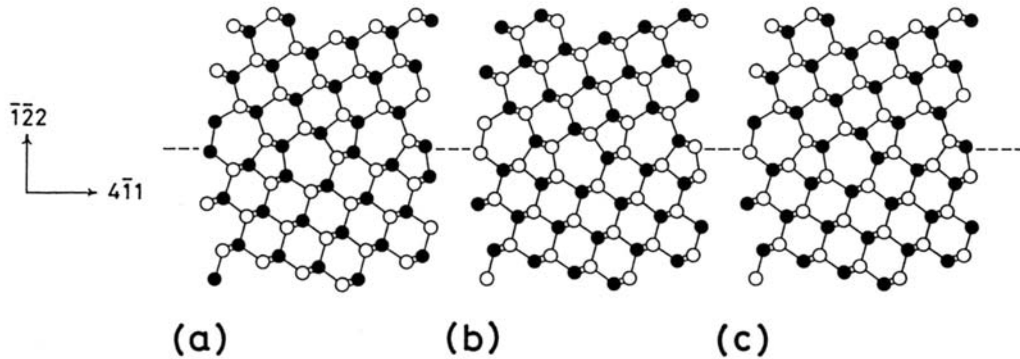

Figure 1: Atomic models of the {122}Σ=9 boundary in SiC. (a)N-type polar, (b) P-type polar, and (c) non-polar interfaces. Atomic positions are projected along the ⟨011⟩ axis. Empty and closed circles represent Si and C atoms, respectively.

We construct a 64-atom supercell. For the non-polar interface, the cell contains two equivalent interfaces with a distance of about $\frac{8}{3}a_0$. For the polar interfaces, it is necessary to stack two different polar interfaces alternately in the same cell by the geometric constraint. However, computations can be executed without any problems because the wrong bonds do not generate any extra carries or deep states in SiC.

Total energies, atomic forces and averaged stresses [10] can be obtained through the electronic-structure calculations of the supercell in the framework of the plane-wave pseudopotential method [11] with the local density-functional theory [12]. We use the conjugate-gradient technique [13] and the optimized pseudopotentials [14] for efficient computations. A plane-wave cutoff energy of 816 eV is used. We use the equilibrium lattice constant by the present theoretical method, which is 98.9% of the experimental one. Two special **k** points per irreducible eighth of the Brillouine zone are used. More details of the scheme are given in [7].

Initially, the stable configurations are obtained through relaxation from the models in Fig. 1. Then we perform the *ab initio* tensile test [6], where uniaxial tensile strain is introduced into the stable configuration. First, the cell is stretched in a small increment in the direction normal to the interface, and the atomic positions are changed by uniform scaling. Second, all the atoms are relaxed through iterative electronic-structure calculations until all the atomic forces are less than a tolerance value. Third, the total energy and stress tensor are calculated. This cycle is iterated until the interfaces are broken. This procedure corresponds to a real slow tensile test at T=0K [6]. For the non-polar interface, two equivalent interfaces in the cell are broken at the same time, because the symmetric property of the cell

is preserved in the calculation. For the polar interfaces, only a weaker interface in the cell is broken.

RESULTS AND DISCUSSION

In the stable configurations, all the interfacial bonds are well reconstructed within small bond distortions. Bond lengths and bond charges of C–C and Si–Si wrong bonds are rather similar to those in bulk diamond and Si. The bond-length and bond-angle distortions of the other Si–C bonds range from –2.9% to +2.9% and from –22.4° to +27.9°, respectively, for the non-polar interface. The bond distortions range from –2.7% to +2.5% and from –13.0° to +24.0° for the P-type polar interface, and from –2.7% to +2.0% and from –20.1° to +22.5° for the N-type polar interface. The boundary energy of the non-polar interface is 1.27 Jm^{-2}, which is very much smaller than that of two surfaces. The averaged boundary energy of the two polar interfaces is a little smaller (1.24 Jm^{-2}).

Fig. 2 shows the stress–strain curves in the tensile tests of the non-polar and polar interfaces. Stresses along the $\langle 411 \rangle$ and $\langle 011 \rangle$ directions parallel to the interfaces are also generated. Strictly speaking, the cell sizes along these two directions should be adjusted in each step so as to remove such stresses. However, this effect is not so serious, because such stresses are relatively small due to the low Poisson's ratio of cubic SiC. From the curves, the Young's modulus of the non-polar interface is 519 GPa, and the averaged value of the polar interfaces is 531 GPa. These are comparable with the bulk SiC value along the $\langle 111 \rangle$ direction, 558 GPa, by a similar first-principles calculation [4].

For the non-polar interface in Fig 2(a), the fracture starts at the strain of 12%. The maximum tensile stress is about 42 GPa at 14%, which is the strength of the non-polar interface. For the polar interfaces in Fig. 2(b), the P-type interface with Si–Si bonds is broken at the strain over 14%, and the N-type interface with C–C bonds is not broken. The maximum stress of about 48 GPa is the strength of the P-type interface. The fracture of this interface occurs rather catastrophically as seen in the sharp decrease of the stress in Fig.2 (b), which is in contrast to the gradual decrease in Fig. 2 (a).

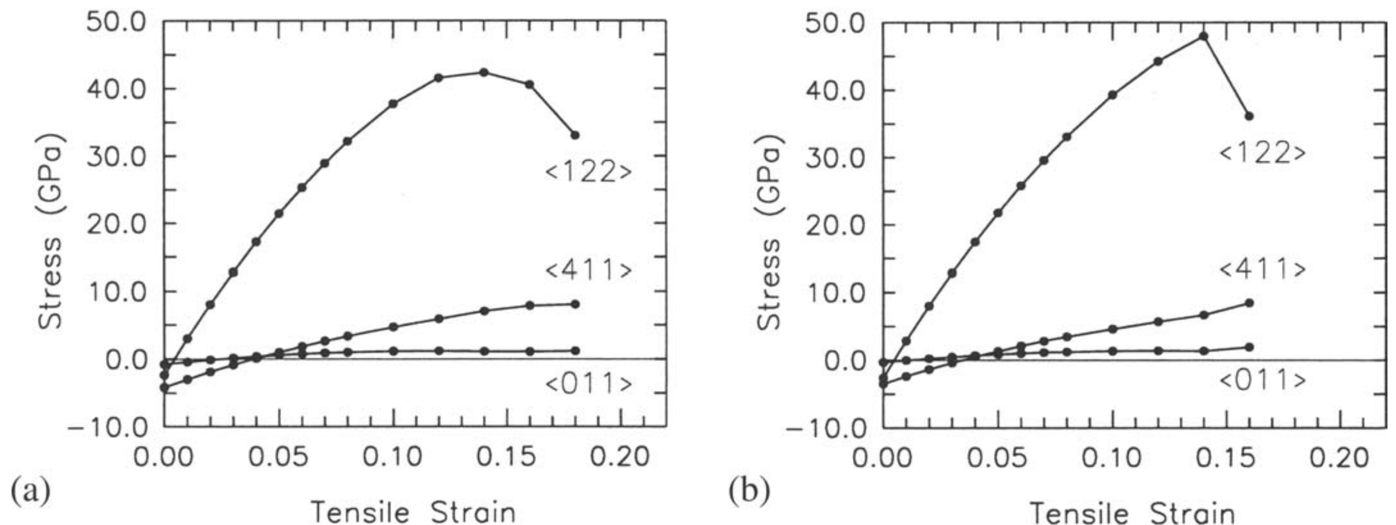

Figure 2: (a) Stress–strain curve of the non-polar interface. (b) Stress–strain curve of the polar interfaces.

The N-type polar interface is the strongest, and the non-polar interface is the weakest among the three interfaces. The tensile strength of these interfaces is very large because of the reconstruction of interfacial bonds. The strength is over 80% of the theoretical strength of bulk SiC along the $\langle 111 \rangle$ direction, 50.8 GPa [4], which is in good agreement with the experimental value of 53.4 GPa for a SiC nanorod [15]. The strength of these interfaces is very much larger than the observed macroscopic tensile strength of SiC ceramics, which is usually less than 1 GPa. In usual ceramics, fracture starts from pre-existing

cracks. Under lower macroscopic stresses, the stress concentration occurs at the crack tip. If the local stress at the crack tip exceeds some critical value, the crack should propagate. The present calculated strength of the interfaces and the bulk crystal should correspond to such critical local stress values for the crack propagation, which dominate the behavior of cracks. From the calculated results, the present interfaces should not act as an initial point of fracture, or not necessarily act as a preferential fracture path.

In the fracture of the non-polar interface shown in Fig. 3, the back Si–C bond of the C–C bond is broken first. This is due to the local stress concentration at the atomic scale caused by the special large strength and short bond length of the C–C bond like a diamond bond. At the tensile strain of 10%, the bond stretchings of the C–C bond and the back Si–C bond are +7.0% and +19.4% against the bond lengths of bulk diamond and SiC, respectively. At the strain of 12% shown in Fig. 3(a), the back bond is suddenly stretched into +27.8%, while the C–C bond shrinks into +6.4%. The C–C bond shrinks much more hereafter. Thus the back Si–C bond has been almost broken at this point.

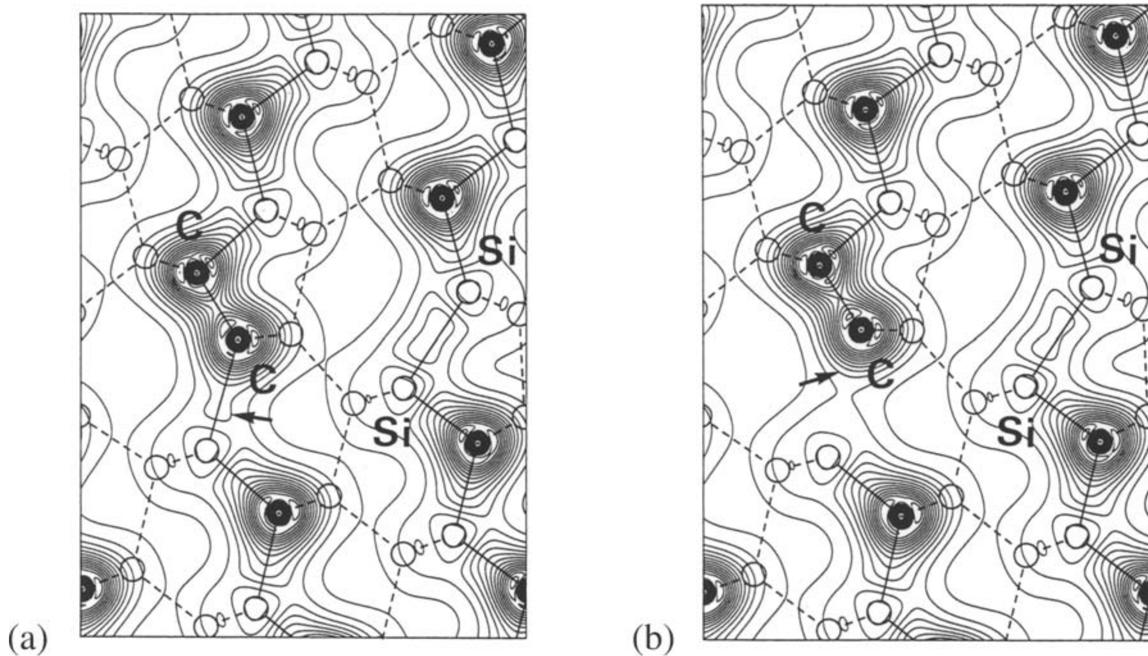

Figure 3: Atomic configurations of the non-polar interface for strains of (a) 12% and (b) 14%. Valence charge densities on the {011} plane are plotted by the contours from 0.015 to 0.275 $\mathrm{a.u.}^{-3}$ with a spacing of 0.02 $\mathrm{a.u.}^{-3}$. Arrows indicate contours of the same value at the back Si–C bond of the C–C bond.

At the strain of 14%, the stretching of the back Si–C bond is +46.3%, and the bond charge clearly disappears as shown in Fig. 3(b). At this point, the fracture proceeds to near interfacial Si–C bonds, where the stretchings of two interfacial bonds are +20.9% and +19.5%. At the strain of 16%, these two bonds are almost broken, and the breaking of the Si–Si bond starts. The fracture proceeds rather continuously from bond to bond. This feature is consistent with the shape of the stress–strain curve in Fig. 2 (a).

From the breaking of the Si–C bonds in the non-polar interface, we can deduce the critical Si–C bond stretching. Once the bond stretching exceeds about 20%, the Si–C bond cannot sustain the stress, and is rapidly stretched and broken. The bond charge clearly disappears whenever the stretching exceeds about 30%. This is consistent with results of bulk SiC [4]. Thus the criterion for the start of interfacial fracture is the generation of Si–C bond stretching over the critical value.

In the tensile test of the polar interfaces, there occurs no remarkable local stress concentration at the interfaces before the strain of 14%, because of the highly symmetric configurations. Thus the supercell is

stretched without any bond breaking till the strain of 14%, which results in the maximum tensile stress larger than that of the non-polar interface. At the strain of 14%, the stretching of the two Si–C bonds at the P-type interface indicated in Fig. 4(a) is +21.3%, which reaches the criterion of the Si–C bond breaking for the first time. The reason why these two Si–C bonds are greatly stretched is that the Si–Si bonds constituting seven-membered rings with these two Si–C bonds are long and easily stretched. At this point, the length of the Si–Si bond is +41.7% against the bulk SiC bond length. On the other hand, the maximum Si–C bond stretching is +17.3% for the N-type interface at this point. Therefore the two Si–C bonds at the P-type interface are broken rapidly during the relaxation at the strain of 16%. This means the breaking of a half of interfacial bond chains sustaining the stress in one period of the interface. Thus the two Si–Si bonds are also broken rapidly just after the Si–C bond breaking in the relaxation at 16%. At the same time, all the bonds at the N-type interface in the supercell shrink. In this way, the fracture of the P-type polar interface occurs rather catastrophically as shown in Fig. 4(b) and Fig. 2(b).

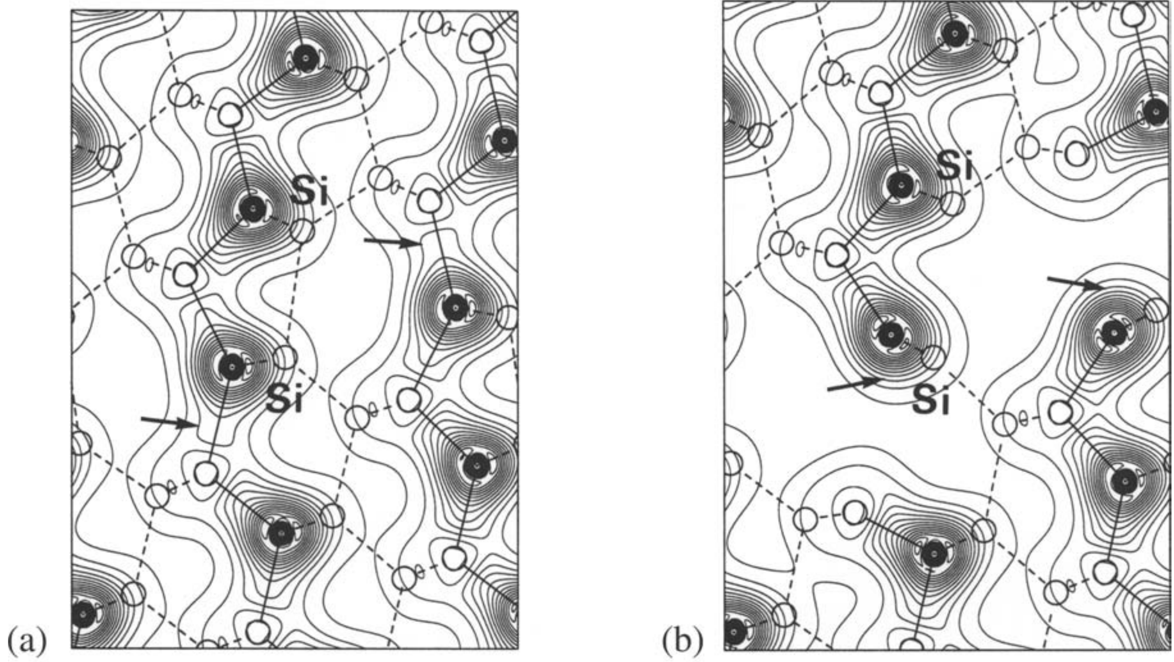

Figure 4: Atomic configurations of the P-type polar interface for strains of (a) 14% and (b) 16%. Arrows indicate contours of the same value at the Si–C bonds breaking first. Note that the Si–Si bond is located on the {011} plane other than that on which the densities are plotted.

The changes in the electronic structure during the tensile test have been examined in detail for the non-polar interface. The valence-band width and the band-gap width are gradually decreased. However, there seem to exist no dramatic changes associated with the bond breaking. The system is semiconducting even after the bond breaking. This feature can be explained as rather continuous changes of occupied and unoccupied weak-bond states into occupied C and unoccupied Si dangling-bond states, respectively, without generating deep gap states. This should be typical of compounds with both covalent and ionic characters.

About the effects of the cell size along the ⟨122⟩ direction, we think that the present cell size is sufficient. This is because the atomic layers in the bulk regions in the present cell seem to behave like a bulk crystal with a uniform expansion along the ⟨122⟩ direction. Concerning the effects of high temperature which are not included in the present calculations, thermal lattice dynamics and electronic excitation are important. The former may reduce the maximum strength, because bond stretchings over the criterion of breaking may occur locally associated with lattice dynamics. The latter may also reduce the strength, although this should be substantial only at very high temperature because of the large band gap.

CONCLUSION

The *ab initio* tensile test has been applied to polar and non-polar interfaces of a coincidence tilt boundary in SiC. The intrinsic tensile strength and fracture have been clarified through the behavior of electrons and atoms based on the density-functional theory. Coincidence tilt boundaries with reconstructed interfacial bonds should have large strength comparable with the bulk crystal, and should not act as an initial point of fracture or a fracture path. However, the kinds and arrangement of Si–Si and C–C wrong bonds seriously affects the strength and features of fracture. It seems that atomic-scale inhomogeneity or singularity by the presence of wrong bonds induces local stress concentration at the atomic scale, which should lower the strength. It is of great interest to apply the present kind of calculations to different kinds of boundaries or boundaries with impurities or dopants. The present kind of calculations are promising tools to investigate the basic mechanical properties of materials interfaces.

ACKNOWLEDGEMENT

The author is grateful to Dr. K. Tanaka and Dr. S. Tanaka for fruiteful discussions. The present study was supported by the Science and Technology Agency of Japan as the project 'Frontier Ceramics'.

REFERENCES

1. Car, R. and Parrinello, M. (1985). *Phys. Rev. Lett.* **55**, 2471.
2. Hohenberg, P. and Kohn, W. (1964). *Phys. Rev.* **136**, B864; Kohn, W. and Sham, J.L. (1965). *ibid.* **140**, A1133.
3. Molteni, C., Francis, G.P., Payne, M.C. and Heine, V. (1996). *Phys. Rev. Lett.* **76**, 1284.
4. Li, W. and Wang, T. (1999). *Phys. Rev. B* **59**, 3993.
5. Pérez, R. and Gumbsch, P. (2000). *Phys. Rev. Lett.* **84**, 5347.
6. Deyirmenjian, V.B., Heine, V., Payne, M.C., Milman, V., Lynden-Bell, R.M. and Finnis, M.W. (1995). *Phys. Rev. B* **52**, 15191.
7. Kohyama, M. (1999). *Phil. Mag. Lett.* **79**, 659.
8. Tanaka, K. and Kohyama, M. (1998). In: *Electron Microscopy 1998, Vol. II*, p.581, Benavides, H.A.C. and Yacamán, M.J. (Eds.), Institute of Physics, Bristol.
9. Kohyama, M., Kose, S., Kinoshita, M. and Yamamoto, R. (1990). *J. Phys.: Condens. Matter* **2**, 7809; Kohyama, M., Kose, S., Kinoshita, M. and Yamamoto, R. (1991). *ibid.* **3**, 7555; Kohyama, M. (1997). *Mater. Chem. Phys.* **50**, 159.
10. Nielsen, O.H. and Martin, R.M. (1985). *Phys. Rev. B* **32**, 3780.
11. Hamann, D.R., Schlüter, M. and Chiang, C. (1979). *Phys. Rev. Lett.* **43**, 1494.
12. Perdew, J.P. and Zunger, A. (1981). *Phys. Rev. B* **23**, 5048.
13. Payne, M.C., Teter, M.P., Allen, D.C., Arias, T.A. and Joannopoulos, J.D. (1992). *Rev. Mod. Phys.* **64**, 1045.
14. Troullier, N. and Martins, J.L. (1991). *Phys. Rev. B* **43**, 1993.
15. Wong, E.W., Sheehan, P.E. and Lieber, C.M. (1997). *Science* **277**, 1971.